RSC Advances

PAPER

View Article Online
View Journal | View Issue

Cite this: *RSC Adv.*, 2022, **12**, 3716

Rational and site-selective formation of coordination polymers consisting of d^{10} coinage metal ions with thiolate ligands using a metal ion-doped polymer substrate†

Takaaki Tsuruoka, *[a] Yuri Miyashita,[a] Ryuki Yoshino,[a] Myu Fukuoka,[a] Shoya Hirao,[a] Yohei Takashima,[a] Aude Demessence[b] and Kensuke Akamatsu[a]

Received 14th January 2022
Accepted 20th January 2022

DOI: 10.1039/d2ra00269h

rsc.li/rsc-advances

Here, we report an interfacial approach for fabricating coordination polymers (CPs) consisting of d^{10} coinage metal ions with thiolate ligands on a polymer substrate. It was found that CPs were selectively formed on the polymer substrate, resulting in the formation of CP-based thin films. In addition, utilizing a mixed metal ion-doped polymer substrate leads to the formation of mixed-metal CP-based films.

1. Introduction

Low-dimensional coordination polymers (CPs) have attracted enormous attention due to their outstanding photophysical properties and unique performance in the optoelectronics field.[1] In particular, CPs consisting of d^{10} coinage metal ions with thiolate ligands have been considered as fundamental building units for nanodevice technologies.[2] A variety of flexible, lightweight, and portable solid-state optoelectronic devices consisting of CPs have been proposed owing to the ease of synthesis of CPs with high crystallinity as well as their unique photoluminescence properties.[3] However, the significant challenges in CP-based thin films should be addressed to realize CP optoelectronics by device integration. The poor processability of CPs considerably limits their applicability, as CP materials exhibit intrinsic instability against a range of process parameters to form the desired shapes and patterns.[4] For example, device fabrication based on the synthesis of CPs in the reaction solution followed by fabrication of CP-based thin films remains difficult to apply because of the degradation of CPs during processes where the CP makes contact with any other chemicals, such as developers and photoresist, which include a number of chemical functionalities that damage the CP upon contact. To address this issue, several approaches for the direct fabrication of CP-based thin films have been proposed, including the layer-by-layer approach,[5] a direct formation on the functionalized substrate,[6] and the replication approach using metal oxide substrates.[7] We have also demonstrated a simple interfacial approach for the construction of CP crystals using metal ion-doped polymer substrates.[8] Recent studies on the development of a synthetic approach for CPs on the substrate have proved the significance of the direct fabrication of CP-based films, and demonstrated that it is an ideal option for a simple and reproducible approach for assembling into CP-based devices. However, considerable efforts have been devoted to the synthesis of various porous CPs (PCPs) and/or metal–organic frameworks-based films. In addition, the preparation of nonporous CP-based films remains challenging and unexplored.

Herein, we demonstrate an interfacial synthetic approach for fabricating CPs comprising d^{10} coinage metals and thiolates on polymer substrates. In this study, we selected a [Cu(*p*-SPhCOOH)]$_n$,[9] [Ag(*p*-SPhCOOH)]$_n$ and mixed-metal [Cu_xAg_{1-x}(*p*-SPhCOOH)]$_n$ CPs.[10] We employed the polyimide substrate bearing cation-exchangeable group by hydrolyzing alkali solutions for precursors and template for CP-based films (Scheme 1). The metal ion-doped polymer substrate led to the selective formation of CPs on the surface and the construction of mixed-metal CPs. In addition, a pattern of polymethyl methacrylate (PMMA) photoresist on a metal ion-doped polymer substrate was fabricated in a positive-type with vacuum ultraviolet (VUV) light illumination,[11] enabling the formation of CP thin films with the desired patterns.

Results and discussion

Scanning electron microscopy (SEM) observations of the obtained samples (Fig. 1A) indicated that CP crystals with a plate shape were densely deposited on the substrate, yielding

[a]*Department of Nanobiochemistry, Frontiers of Innovative Research in Science and Technology (FIRST), Konan University, 7-1-20 Minatojimaminami, Chuo-ku, Kobe 650-0047, Japan. E-mail: tsuruoka@konan-u.ac.jp*

[b]*Univ Lyon, Université Claude Bernard Lyon 1, Institut de Recherches sur la Catalyse et l'Environnement de Lyon (IRCELYON), UMR 5256, CNRS, Villeurbanne, France*

† Electronic supplementary information (ESI) available: Experimental; effect of hydrolysis time on amounts of doped copper ion; luminescent property of the obtained samples; formation of [Ag(*p*-SPhCOOH)]$_n$ CP and mixed-metal [Cu_xAg_{1-x}(*p*-SPhCOOH)]$_n$ CPs on substrate; high-resolution SEM image and XRD pattern of patterned-[Cu(*p*-SPhCOOH)]$_n$ CP on substrate. See DOI: 10.1039/d2ra00269h

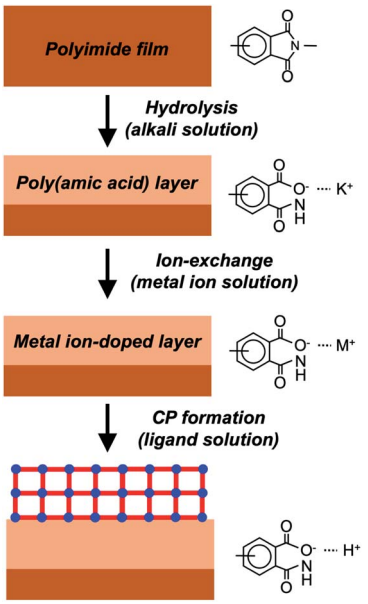

Scheme 1 Schematic illustration of the developed interfacial approach for formation of $[M(p\text{-SPhCOOH})]_n$ (M = Cu or Ag) CPs on a substrate.

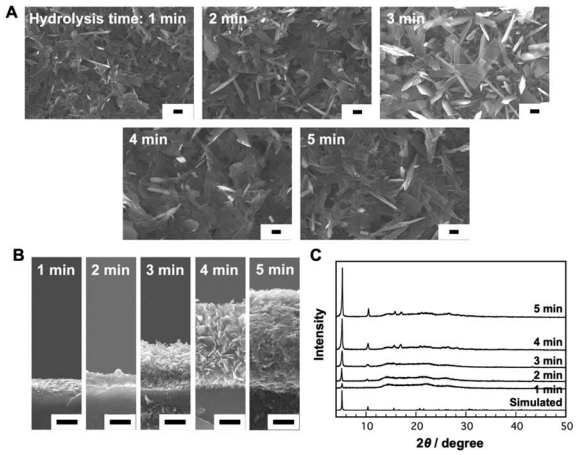

Fig. 1 (A) SEM images, (B) cross-sectional SEM images, and (C) XRD patterns of the obtained samples using metal ion-doped substrate prepared by different hydrolysis times. Scale bars: 1 μm.

continuous CP-based films. Importantly, as seen in Fig. 1B, the thickness of CP-based films varied with the hydrolysis time of the substrate. It is well-known that polyimide is readily hydrolyzed to poly(amic acid) by treatment of an aqueous alkali solution with high concentration.[12] Longer hydrolysis times led to a higher degree of hydrolysis, causing an increase in the number of potassium ions in proportion to the hydrolysis time. After ion exchange, the number of Cu^{2+} ions was almost half that of the potassium ions adsorbed initially, indicating that the incorporation of the desired ions can be achieved through the ion-exchange reaction (Fig. S1†). Under the present experimental conditions (hydrolysis time: 1–5 min), the thickness of CP-based films could be controlled in the 0.6–4.8 μm range. X-ray diffraction (XRD) analysis of the obtained samples clearly demonstrated the formation of $[Cu(p\text{-SPhCOOH})]_n$ CPs (Fig. 1C and S2†); all peaks of the obtained samples were assigned to $[Cu(p\text{-SPhCOOH})]_n$ CP peaks (simulation) and the halo pattern of polyimide.[8,9] Moreover, the sharp diffraction peaks of the obtained samples indicated that the obtained CPs consisted of $[Cu(p\text{-SPhCOOH})]_n$ CPs with high crystallinity. The $[Cu(p\text{-SPhCOOH})]_n$ CPs exhibited characteristics of ligand-to-metal charge transfer (LMCT) and ligand-to-metal–metal charge transfer (LMMCT).[9] To investigate the luminescence properties of the obtained composite material, the film was characterized by fluorescence spectrometry (Fig. S3†). The luminescence spectra of the obtained CPs on the substrate revealed that the luminescence consisted of three peaks at approximately 425, 475, and 598 nm. Among these peaks, the two peaks observed at shorter wavelengths are attributed to ligand emission (Fig. S4†), and the peaks around 598 nm are caused by the charge transfer emission of the CPs. The intensity of the luminescent peaks increased with increasing hydrolysis time, indicating that a larger amount of CPs was formed on the substrate. This result was in good agreement with the cross-sectional SEM observation of the thickness of the obtained CPs on the substrate (Fig. 1B).

To evaluate the impact of the concentration of organic ligands on the surface morphology of the $[Cu(p\text{-SPhCOOH})]_n$ CPs, the concentration of *p*-HSPhCOOH molecules was varied in the range of 1–50 mM, while the number of adsorbed Cu^{2+} ions was maintained constant at 1000 nmol cm^{-2} (hydrolysis time = 3 min). Fig. 2 shows the surface morphologies of the samples prepared with different ligand concentrations. When the reaction was conducted at a concentration of 1 mM, samples with a plate morphology were sparsely formed on the substrate, and the XRD patterns clearly indicated the formation of the $[Cu(p\text{-SPhCOOH})]_n$ CPs. This result suggested that the concentration of ligand molecules below 1 mM was insufficient to fabricate densely packed CP films on the substrate. In contrast, when the ligand concentration was set to 2 mM or higher, the SEM images demonstrated that crystals with a plate morphology were densely formed on the substrate. In addition, as the ligand

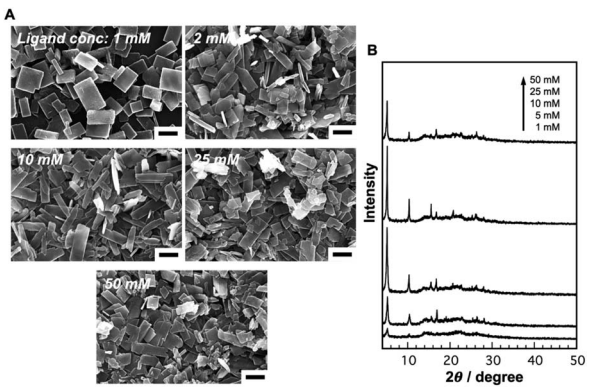

Fig. 2 (A) SEM images and (B) XRD patterns of the obtained samples prepared using different ligand concentrations. Scale bars: 1 μm.

concentration increased, the crystal size slightly decreased (major axis = 1.8 μm, minor axis = 1.0 μm at 2 mM; major axis = 1.7 μm, minor axis = 0.5 μm at 50 mM), suggesting that the nucleation preferentially occurred in the early stage of the reaction. From the XRD pattern of the obtained samples (Fig. 2B), several sharp peaks were observed, and the peak intensities of the samples obtained using higher ligand concentrations were more pronounced. This result indicated that a high ligand concentration could lead to the formation of densely packed CP films on the substrate. However, the intensity of the peaks of the samples prepared at a ligand concentration of 50 mM was lower than that of the samples prepared at a ligand concentration of 25 mM. Moreover, the $[Cu(p\text{-}SPhCOOH)]_n$ CPs were also formed in the solution, implying the optimal ligand concentration for selective CP formation on the substrate of 25 mM in the present approach.

The present approach was also applied to construct the $[Ag(p\text{-}SPhCOOH)]_n$ CP. To form the $[Ag(p\text{-}SPhCOOH)]_n$ CP, the Ag^+-doped polymer films was utilized as the substrates. SEM images of the obtained samples showed that plate-like crystals were formed on the substrate, resulting in the formation of CP crystal films. In addition, XRD analysis of the obtained crystals clearly demonstrated the formation of $[Ag(p\text{-}SPhCOOH)]_n$ crystals (Fig. S5†).[10] The obtained crystals exhibited only ligand emission. This result was consistent with previous report.[9]

Mixed-metal CP crystals can also be readily obtained in a wide range of synthetic compositions by varying the concentration of the metal ion dopant in the polymer substrate. Prior to synthesizing mixed-metal CP crystals, ion-codoped precursor films were prepared by immersing hydrolyzed polyimide films in an aqueous solution containing both silver nitrate and copper nitrate at 25 °C. Quantitative analysis of the ion-doped polymer films by inductively coupled plasma (ICP) spectroscopy revealed that the dopant ion concentrations in the polymer could be readily controlled by changing the concentrations of the doped ions, which varied with the initial concentrations in the aqueous solution (Fig. S6†). In addition, the total amount of doped ions increased with an increase in the fraction of Ag ions in the solution, because Ag ions are monovalent (Cu ions: divalent) and the incorporation of metal ions in the polymer substrate can be achieved through the ion-exchange of monovalent K ions with monovalent Ag ions in a 1 : 1 stoichiometric ratio. To gain insight into the distributions of the doped metal ions in the polyimide films, we performed energy-dispersive X-ray spectroscopy (EDX) analysis of the obtained metal ion-doped films. The doped Ag and Cu ions were uniformly distributed in the films (Fig. S7†). Based on these results, it was possible to systematically control the relative amounts and distributions of the doped metal ions in the precursor films by adjusting the initial ion concentrations in the aqueous solution.

SEM images of mixed-metal $[Cu_xAg_{1-x}(p\text{-}SPhCOOH)]_n$ CP crystals obtained by using polymers with different Ag and Cu ion contents indicated that plate-like crystals could be obtained (Fig. 3A). The plate-like morphology of the obtained crystals was almost the same as that of mononuclear CP crystals. The corresponding XRD patterns of the mixed-metal CP crystals are

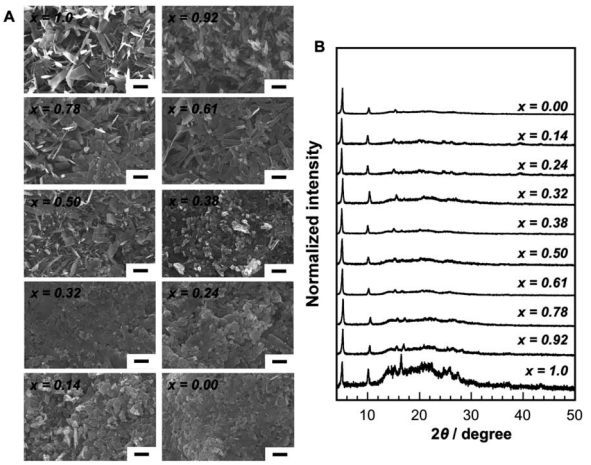

Fig. 3 (A) SEM images and (B) XRD patterns of $[Cu_xAg_{1-x}(p\text{-}SPhCOOH)]_n$ CPs prepared using polyimide films with different amounts of adsorbed copper and silver ions. Scale bars: 1 μm.

presented in Fig. 3B. The obtained mixed-metal $[Cu_xAg_{1-x}(p\text{-}SPhCOOH)]_n$ CP crystals were isostructural with the mononuclear $[Cu(p\text{-}SPhCOOH)]_n$ and $[Ag(p\text{-}SPhCOOH)]_n$ CPs. ICP measurements were performed on the mixed-metal CP crystals after stripping them from their substrates to determine the composition of the obtained crystals. Their composition was found to be consistent with that of ion-co-doped polymer substrates, suggesting that the co-doped Cu and Ag ions were incorporated into the mixed-metal CP crystals. This result indicates that the composition of mixed-metal CP crystals can be readily controlled by tuning the concentration of the co-doped cations in the polymer substrates.

Subsequently, the patterning process based on the present approach combined with photolithography can be applied to achieve the site-selective growth of $[Cu(p\text{-}SPhCOOH)]_n$ CP crystals. Since PMMA is known as a negative-tone resist through VUV photolithography,[11] we selected this polymer to demonstrate direct patterning of CP crystals on the substrate. Fig. 4 shows the SEM images of the samples prepared using PMMA-patterned ion-doped substrates. The formation of $[Cu(p\text{-}SPhCOOH)]_n$ CP patterns on the substrate was clearly observed without the occurrence of film cracks. A high-magnification SEM image of the obtained samples indicated that plate-like CP crystals formed a dense network on the substrate with no PMMA resist, which resulted in the formation of CP patterns

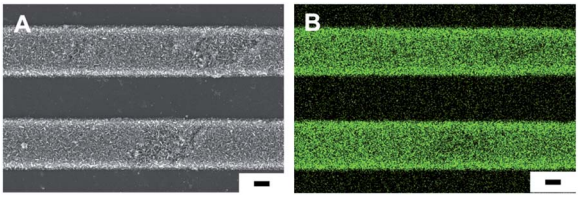

Fig. 4 (A) SEM image and (B) EDX mapping of Cu element of the patterned $[Cu(p\text{-}SPhCOOH)]_n$ CP crystals on the substrate. Scale bar: 1 μm.

(Fig. S8A†). To verify that the formed material was indeed a $[Cu(p\text{-SPhCOOH})]_n$ CP, XRD analysis was performed. All the peaks matched the simulated peaks of $[Cu(p\text{-SPhCOOH})]_n$ CP, indicating that the obtained patterns consisted of a $[Cu(p\text{-SPhCOOH})]_n$ CP with high crystallinity (Fig. S8B†). These results confirmed that patterns consisting of well-defined $[Cu(p\text{-SPhCOOH})]_n$ crystals were successfully prepared by a one-pot approach based on *in situ* CP growth.

Conclusions

In summary, we presented a simple and versatile approach for constructing d^{10} coinage metal ion-thiolate CPs by exploiting an interfacial synthetic approach using metal ion-doped polymer substrates. We found that the $[Cu(p\text{-SPhCOOH})]_n$ CP crystals were densely formed on the substrate, and the thickness of CP-based films increased with an increase in the amount of doped metal ions. We showed that the use of a mixed-metal ion-doped polymer substrate resulted in the formation of mixed-metal CP crystals. In addition, the composition of metal ions in CP crystals can be controlled by adjusting the composition of the doped metal ions in the polymer substrates. Site-selective formation of the $[Cu(p\text{-SPhCOOH})]_n$ CP crystals can be achieved by an interfacial synthetic approach combined with a photolithographic technique, resulting in the formation of a CP crystal pattern. This work highlights the potential of the construction and patterning approach for CP crystal-based films, acting as new optoelectronic devices.

Author contributions

Y. M., R. Y., M. F. and S. H. performed the synthesis experiments. T. T. conceived the experiments and supervised the project. Y. T., A. D., K. A. and T. T. analyzed all data and discussed. All authors contributed to the preparation of the manuscript.

Conflicts of interest

There are no conflicts to declare.

Acknowledgements

This work was supported by JSPS KAKENHI Grant Number 21H05109. We would like to than Editage (https://www.editage.com) for English language editing.

Notes and references

1 A. Y. Robin and K. M. Fromm, *Coord. Chem. Rev.*, 2006, **250**, 2127–2157; W. L. Leong and J. J. Vittal, *Chem. Rev.*, 2011, **111**, 688–764; M. Yadav, A. Bhunia, S. K. Jana and P. W. Roesky, *Inorg. Chem.*, 2016, **55**, 2701–2708; A. Karmakar, G. M. D. M. Rúbio, C. M. Fátima, G. da Silva, S. Hazra and A. J. L. Pombeiro, *Cryst. Growth Des.*, 2015, **15**, 4185–4197; T. Yamada, K. Otsubo, R. Makiura and H. Kitagawa, *Chem. Soc. Rev.*, 2013, **42**, 6655–6669; J. A. Hurd, R. Vaidhyanathan, V. Thangadurai, C. I. Ratcliffe, I. L. Moudrakovski and G. K. H. Shimizu, *Nat. Chem.*, 2009, **1**, 705–710; D. Umeyama, S. Horike, M. Inukai and S. Kitagawa, *J. Am. Chem. Soc.*, 2013, **135**, 11345–11350; B. Zhao, Z.-Y. Chen, P. Cheng, D.-Z. Liao, S.-P. Yan and Z.-H. Jiang, *J. Am. Chem. Soc.*, 2004, **126**, 15394–15395; G.-Y. Wang, L.-L. Yang, Y. Li, H. Song, W.-J. Ruan, Z. Chang and X.-H. Bu, *Dalton Trans.*, 2013, **42**, 12865–12868.

2 O. Veselska and A. Demessence, *Coord. Chem. Rev.*, 2018, **355**, 240–270; L. Han, M. Hong, R. Wang, B. Wu, Y. Xu, B. Lou and Z. Lin, *Chem. Commun.*, 2004, 2578–2579; J.-S. Shen, D.-H. Li, M.-B. Zhang, J. Zhou, H. Zhang and Y.-B. Jiang, *Langmuir*, 2011, **27**, 481–486.

3 S.-L. Zhang, J.-H. Yang, X.-L. Yu, X.-M. Chen and W.-T. Wong, *Inorg. Chem.*, 2004, **43**, 830–838; C. Seward, J. Chan, D. Song and S. Wang, *Inorg. Chem.*, 2003, **42**, 112–1120; H. Tan, B. Liu and Y. Chen, *ACS Nano*, 2012, **6**, 10505–11511; W.-G. Lu, J.-Z. Gu, L. Jiang, M.-Y. Tan and T.-B. Lu, *Cryst. Growth Des.*, 2008, **8**, 192–199; R. G. Xiong, J.-L. Zuo, X.-Z. You, B. F. Abrahams, Z.-P. Bai, C.-M. Che and H.-K. Fun, *Chem. Commun.*, 2000, 2061–2062; X. Feng, R. Li, L. Wang, S. W. Ng, G. Qin and L. Ma, *CrystEngComm*, 2015, **17**, 7878–7887; Y. Gong, J. Li, J. Qin, T. Wu, R. Cao and J. Li, *Cryst. Growth Des.*, 2011, **11**, 1662–1674.

4 W. Cho, J. L. Hee and M. Oh, *J. Am. Chem. Soc.*, 2008, **130**, 16943–16946; H. Ming, N. L. K. Torad, Y.-D. Chiang, K. C.-W. Wu and Y. Yamauchi, *CrystEngComm*, 2012, **14**, 3387–3396; Q. Liu, J. M. Yang, L.-N. Jin and W.-Y. Sun, *Chem.–Eur. J.*, 2014, **20**, 14783–14789.

5 O. Shekhah, H. Wang, D. Zacher, R. A. Fischer and C. Wöll, *Angew. Chem., Int. Ed.*, 2009, **48**, 5038–5041; B. Liu, O. Shekhah, H. K. Arslan, J. Liu, C. Wöll and R. A. Fischer, *Angew. Chem., Int. Ed.*, 2012, **51**, 807–810; K. Otsubo, T. Haraguchi, O. Sakata, A. Fujiwara and H. Kitagawa, *J. Am. Chem. Soc.*, 2012, **134**, 9605–9608.

6 J. Yao, D. Dong, D. Li, L. He, G. Xu and H. Wang, *Chem. Commun.*, 2011, **47**, 2559–2561; H. T. Kwon and H.-K. Jeong, *J. Am. Chem. Soc.*, 2013, **135**, 10763–10768; P. Falcaro, K. Okada, T. Hara, K. Ikigaki, Y. Tokudome, A. W. Thornton, A. J. Hill, T. Williams, C. Doonan and M. Takahashi, *Nat. Mater.*, 2017, **16**, 342–348.

7 Z. Dai, S. Paradeep, J. Zhu, W. Xie, H. F. Barton, Y. Si, B. Ding, J. Yu and G. N. Parsons, *Adv. Mater. Interfaces*, 2021, **8**, 2101178; A. S. Hall, A. Kondo, K. Maeda and T. E. Mallouk, *J. Am. Chem. Soc.*, 2013, **135**, 16276–16279; J. Reboul, S. Furukawa, N. Horike, M. Tsotsalas, K. Hirai, H. Uehanara, M. Kondo, N. Louvain, O. Sakata and S. Kitagawa, *Nat. Mater.*, 2012, **11**, 717–723.

8 T. Tsuruoka, M. Kumano, K. Mantani, T. Matsuyama, A. Miyanaga, T. Ohhashi, Y. Takashima, H. Minami, T. Suzuki, K. Imagawa and K. Akamatsu, *Cryst. Growth Des.*, 2016, **16**, 2472–2476; T. Tsuruoka, K. Mantani, A. Miyanaga, T. Matsuyama, T. Ohhashi, Y. Takashima and K. Akamatsu, *Langmuir*, 2016, **32**, 6068–6073; T. Ohhashi, T. Tsuruoka, S. Fujimoto, Y. Takashima and K. Akamatsu, *Cryst. Growth Des.*, 2018, **18**, 402–408.

9 O. Veselska, L. Cai, D. Podbevšek, G. Ledoux, N. Guillou, G. Pilet, A. Fateeva and A. Demessence, *Inorg. Chem.*, 2018, **57**, 2736–2743.

10 O. Veselska, C. Dessal, S. Melizi, N. Guillou, D. Podbevšek, G. Ledoux, E. Elkaim, A. Fateeva and A. Demessence, *Inorg. Chem.*, 2019, **58**, 99–105.

11 J.-K. Chen, F.-H. Ko and F.-C. Chang, *Adv. Funct. Mater.*, 2005, **15**, 1147–1154; T. Tsuruoka, T. Matsuyama, A. Miyanaga, T. Ohhashi, Y. Takashima and K. Akamatsu, *RSC Adv.*, 2016, **6**, 77297–77300.

12 S. Ikeda, K. Akamatsu, H. Nawafune, T. Nishino and S. Deki, *J. Phys. Chem. B*, 2004, **108**, 15599–15607.